





The chondrite breccia of Antonin (L4-5)—A new meteorite fall from Poland with a heterogeneous distribution of metal

Addi BISCHOFF ^{1*}, Markus PATZEK ¹, Stefan T. M. PETERS^{2,3}, Jean-Alix BARRAT^{4,5}, Tommaso DI ROCCO², Andreas PACK², Samuel EBERT ¹, Christian A. JANSEN ¹, and Kryspin KMIECIAK⁶

¹Institut für Planetologie, University of Münster, Wilhelm-Klemm-Str. 10, D-48149 Münster, Germany

²Universität Göttingen, Geowissenschaftliches Zentrum, Goldschmidtstr. 1, D-37077 Göttingen, Germany

³Museum der Natur Hamburg – Mineralogie, LIB, Grindelallee 48, D-20146 Hamburg, Germany

⁴University of Brest, CNRS, IRD, Ifremer, LEMAR, F-29280 Plouzané, France

⁵Institut Universitaire de France, Paris 75005, France

⁶Olsza 2, 63-100 Śrem, Kraków, Poland

*Corresponding author. E-mail: bischoa@uni-muenster.de

(Received 16 May 2022; revision accepted 11 July 2022)

Abstract—On July 15, 2021, a huge fireball was visible over Poland. After the possible strewn field was calculated, the first and so far only sample, with a mass of 350 g, was discovered 18 days after the fireball event. The Antonin meteorite was found August 3, 2021, on the edge of a forest close to a dirt road near Helenow, a small suburb of the city of Mikstat. The rock is an ordinary chondrite breccia and consists of equilibrated and recrystallized lithologies. The boundaries between different fragments are difficult to detect, and the lithologies are of petrologic type 5 and type 4. The rock is moderately shocked (S4) and contains local impact melt areas and thin shock veins. The low-Ca pyroxene and olivine are equilibrated (Fs_{20.6} and Fa_{24.0}, respectively), typical of L chondrites. The L chondrite classification is also supported by O isotope data and the results of bulk chemical analysis. The Ti isotope characteristics confirm that Antonin is related to the noncarbonaceous (NC) meteorites. One of the studied thin sections shows an unusual metal–chondrule assemblage, perhaps indicating that the metal in the chondrite is heterogeneously distributed, which is, however, not clearly visible in the element abundances.

INTRODUCTION

The Meteoritical Bulletin Database (The Meteoritical Bulletin, 2022) includes 35 recorded entries for meteorites from Poland, including 8 entries for doubtful or pseudometeorites and 1 meteorite crater (Morasko). Among these meteorites, 12 (and 2 doubtful) rocks are listed as observed falls. The last meteorite fall, “Antonin,” fell in 2021 and is the object of detailed studies in this work. Antonin has been classified as an L5 chondrite with a shock degree of S3 (The Meteoritical Bulletin, 2022), although the sample was described as “moderately shocked,” which would be consistent with the shock stage of S4 in the classification scheme of Stöffler et al. (1991, 2018). First results about Antonin are presented by Shrbený et al. (2022) and Krzesińska

et al. (2022) showing, for example, homogeneous and chemically equilibrated olivine (Fa_{24.4}) and pyroxene (Fs_{20.9}) with rare plagioclase and the presence of shock melt pockets.

Considering the fall of Antonin, a huge, impressive fireball was observed at 05:00:11 in the morning over Poland on July 15, 2021. After a possible strewn field was calculated, the search for meteorite samples began in late July. So far, only one sample—totaling 350 g—was discovered 18 days after the fireball event. The Antonin meteorite was found August 3, 2021, on the edge of a forest close to a dirt road near Helenow, a small suburb of Mikstat, south of Ostrowo.

In this study, we report in-depth findings on the mineralogy and chemistry of Antonin accompanied by isotopic analyses of O and Ti.

Samples and Analytical Procedures

A thin slice of 2.6×1.5 cm was used for this study (Fig. 1). Two thin sections of Antonin (PL22011 and PL22012) with a total area of ~ 160 mm² were studied by optical and electron microscopy. An Axiophot polarizing microscope (Fa. ZEISS) at the Institut für Planetologie (University of Münster) was used for optical microscopy in transmitted and reflected light.

A JEOL 6610-LV scanning electron microscope (SEM) at the University of Münster was used to study the meteorites' fine-grained textures and to identify the different mineral phases. The INCA analytical program provided by Oxford Instruments was used for the energy-dispersive spectrometry (EDS).

Quantitative mineral analyses were obtained using the JEOL JXA 8530F electron probe micro-analyzer (EPMA) at the Institut für Mineralogie (University of Münster), which was operated at 15 kV and a probe current of 15 nA. Natural and synthetic standards were used for wavelength-dispersive spectrometry (WDS). As standards for mineral analyses, we used jadeite (Na), kyanite (Al), sanidine (K), chromium oxide (Cr), San Carlos olivine (Mg), hypersthene (Si), diopside (Ca), rhodonite (Mn), rutile (Ti), fayalite (Fe), apatite (P), celestine (S), Co-metal (Co), and nickel oxide (Ni).

Bulk Chemical Analyses

A bulk sample of 0.55 g from Antonin was crushed and homogenized, and about 170 mg from this powder was used for analyses at the University of Brest (Plouzané, France). The chemical compositions of the Renchen (Bischoff, Barrat, et al., 2019) and Antonin bulk samples were obtained using inductively coupled plasma atomic emission spectrometry (ICP-AES; for Al, Fe, Mn, Mg, Na, Cr, Co, and Ni) and inductively coupled plasma sector field mass spectrometry (ICP-SFMS). At the chondritic level, the concentration reproducibility is generally much better than 5%. Further details are presented in Barrat et al. (2012, 2015, 2016).

Oxygen Isotope Analyses

The oxygen isotope compositions are an important tool in the classification of meteorites (e.g., Clayton et al., 1976). The compositions of three chips (2.078, 2.171, and 1.998 mg) from Antonin were analyzed by means of laser fluorination in combination with a gas source mass spectrometer. Details of the analytical procedures are given by Pack et al. (2016) and Peters et al. (2020; also, compare Herwartz et al., 2014; Pack & Herwartz, 2014; Pack et al., 2017). The individual chips were analyzed in one session. The $\delta^{17}\text{O}$ and $\delta^{18}\text{O}$ values are reported on the Vienna Standard Mean Ocean Water (VSMOW) scale, and the $\Delta^{17}\text{O}$ is defined here as:

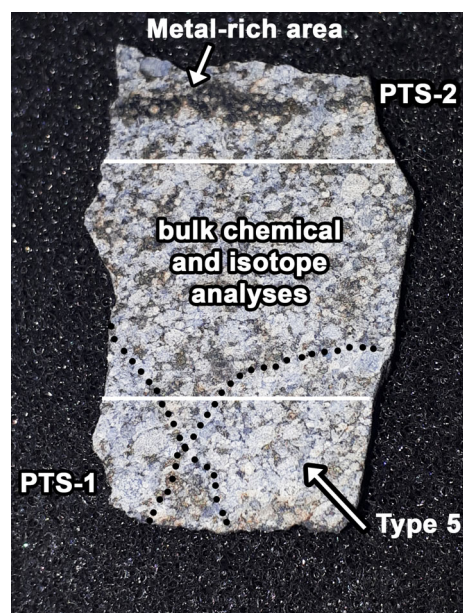


Fig. 1. Sample of Antonin used in this study. Two thin sections were prepared, one from the upper part with the metal-rich area (PTS-2; PL22012) and one from the lower part (PTS-1; PL22011), which mainly contains recrystallized type 5 lithologies as marked. The chemical and isotopic studies were done on the material in the central part of the sample. (Color figure can be viewed at wileyonlinelibrary.com.)

$$\Delta^{17}\text{O} = 1000 \ln\left(\frac{\delta^{17}\text{O}}{1000} + 1\right) - 0.528 \times 1000 \ln\left(\frac{\delta^{18}\text{O}}{1000} + 1\right).$$

To anchor $\delta^{17}\text{O}$ on the VSMOW scale, we used a $\Delta^{17}\text{O}$ value for San Carlos olivine of -0.052‰ (average value of Pack et al., 2016; Sharp et al., 2016; and Wostbrock et al., 2020). Estimated measurement uncertainties are $\pm 0.1\text{‰}$ for $\delta^{18}\text{O}$ and $\pm 0.01\text{‰}$ for $\Delta^{17}\text{O}$, based on replicate analyses of the San Carlos olivine standard (1 SD).

Ti Purification and Isotopic Measurements

After homogenization in an agate mortar, 51 mg of fine-grained Antonin bulk sample powder was digested in a 15 mL Savillex Teflon vial with a mixture of concentrated HF–HNO₃ (3:1, 4 mL) on a hotplate at 190°C for 4 days followed by aqua regia (3:1 HCl–HNO₃, 4 mL) at 140 °C for 2 days. As in our previous Ti isotope studies (e.g., Ebert et al., 2018; Gerber et al., 2017; Render et al., 2019), purification of Ti broadly followed the method of Zhang et al. (2011), which employs a two-stage ion-exchange chromatography with precleaned TODGA (50–100 mesh) and AG1-X8 (200–400 mesh, chloride form) resins. The chemistry yield was $>98\%$ as determined on small aliquots (0.5%) using a quadrupole inductively coupled plasma mass spectrometer (ICP-MS).

Titanium isotope measurements were performed using the Thermo Scientific Neptune *Plus* multicollector ICP-MS at the Institut für Planetologie in Münster in medium resolution mode, based on the methods of Zhang et al. (2011), Gerber et al. (2017), and Burkhardt et al. (2019). Analyte solutions containing $\sim 300 \text{ ng g}^{-1}$ Ti were introduced through a Cetac Aridus II desolvating system, resulting in an $\sim 3.6 \times 10^{-10}$ A ion beam on ^{48}Ti . Measurements consisted of a 30 s baseline (deflected beam) followed by 40 isotope ratio measurements of 4.2 s each. Instrumental mass bias was corrected using the exponential law and internal normalization to $^{49}\text{Ti}/^{47}\text{Ti} = 0.749766$ (Niederer et al., 1981). Titanium isotope anomalies are reported as parts per 10,000 deviation (ϵ -notation) from the terrestrial OL-Ti (Millet & Dauphas, 2014) bracketing standard. Analytical uncertainties are reported as Student's t -distribution 95% confidence intervals based on repeated analyses ($n = 5$).

RESULTS

Details on the Calculated Strewn Field and Characterization of the Search Area

The meteoroid entered the atmosphere early in the morning coming from the west-northwest moving to the

east-southeast. The suggested strewn field has a length of about 7 km with a width of approximately 2 km in the northwest and 1 km in the southeast (Fig. 2). The calculated strewn field is (by far) mainly located in the area of Mikstat. Since the first stone was also found in the Mikstat area, it is very surprising that the rock was officially named “Antonin.”

Two of the authors (K. K. and A. B.) spent many days in the calculated strewn field. The western part is dominated by pine forests growing on partly sandy ground (Fig. 3a). The central area of the strewn field is characterized by a mixture of meadows, pine forests, and farmland (Fig. 3). At the very end of the strewn field in the east, there is a very lush forest resembling a thicket, which was hard to enter.

The Find Location

The first sample was found in the southwestern part of the calculated strewn field having the coordinates of $51^{\circ}30'48.473''\text{N}$, $17^{\circ}54'17.078''\text{E}$ (see Fig. 4). On August 3, 2021, one of the authors (K. K.) and three other persons visited the strewn field again after several days of searching for a sample without any success. The car was parked on a small road close to a forest. Around 2 pm, after a walk of several meters, a “stone” was noticed that looked like a basalt and was quite dark in appearance.



Fig. 2. The strewn field as calculated by Pavel Spurný, Lukáš Shrbený, and Jiří Borovička (Ondřejov, CZ) is mainly located in the area of Mikstat. The red dot marks the position of the first sample that was found in Helenów, a suburb of Mikstat. The neighboring village is Antonin with about 500 residents. Source of base map: Google Earth. Original figure taken from: https://www.asu.cas.cz/meteor/bolid/2021_07_15/. (Color figure can be viewed at wileyonlinelibrary.com.)



Fig. 3. Typical images of the landscape of the Antonin strewn field (a–d) south of the city of Mikstat close to the suburb of Helenow in the southwest and Przedborów in the east of the suggested strewn field. (Color figure can be viewed at [wileyonlinelibrary.com](https://onlinelibrary.wiley.com/doi/10.1111/maps.13905).)

The retrieved stone was dirty due to attached soil, traces of grass, and some coniferous resin. Based on the appearance of the rock having one broken (gray) side and the dark fusion crust elsewhere, it was immediately clear: “It is a meteorite! ... an amazing experience to be the first touching this extraterrestrial traveler.” Due to the presence of resin at the surface, it is very likely that the meteorite hit a tree before landing on the dirt road.

Mineralogy

The two thin sections prepared from two different areas of a small slice (Fig. 1) show that the rock is a breccia and consists of equilibrated and recrystallized lithologies (Fig. 5). The boundaries of the fragments are difficult to detect, and both areas are related to rocks of petrologic type 5 and type 4 (or 4/5). Both lithologies show a recrystallized texture but still have clearly

visible chondrules (Figs. 5 and 6). When comparing the mineralogy of the two thin sections, it is obvious that the metal abundance is heterogeneously distributed in Antonin. Thin section PL22012 contains a large metal-rich area (see below), resembling a metal band, shown in the upper part of Fig. 1.

Different types of chondrules are well preserved (Fig. 6). Barred olivine (BO), radial pyroxene (RP), and cryptocrystalline (C) chondrules are especially easily recognized, whereas porphyritic chondrules are less easy to detect, since they easily merge with the matrix due to metamorphic recrystallization. Some Al-rich chondrules are rich in Na_2O (Fig. 6e,f) (e.g., Bischoff & Keil, 1983a, 1983b, 1984; Ebert & Bischoff, 2016a).

Olivine is by far the most abundant phase and homogeneous in composition throughout the two polished sections. The mean composition of 201 analyzed olivines is $\text{Fa}_{24.0 \pm 0.5}$ with a compositional range

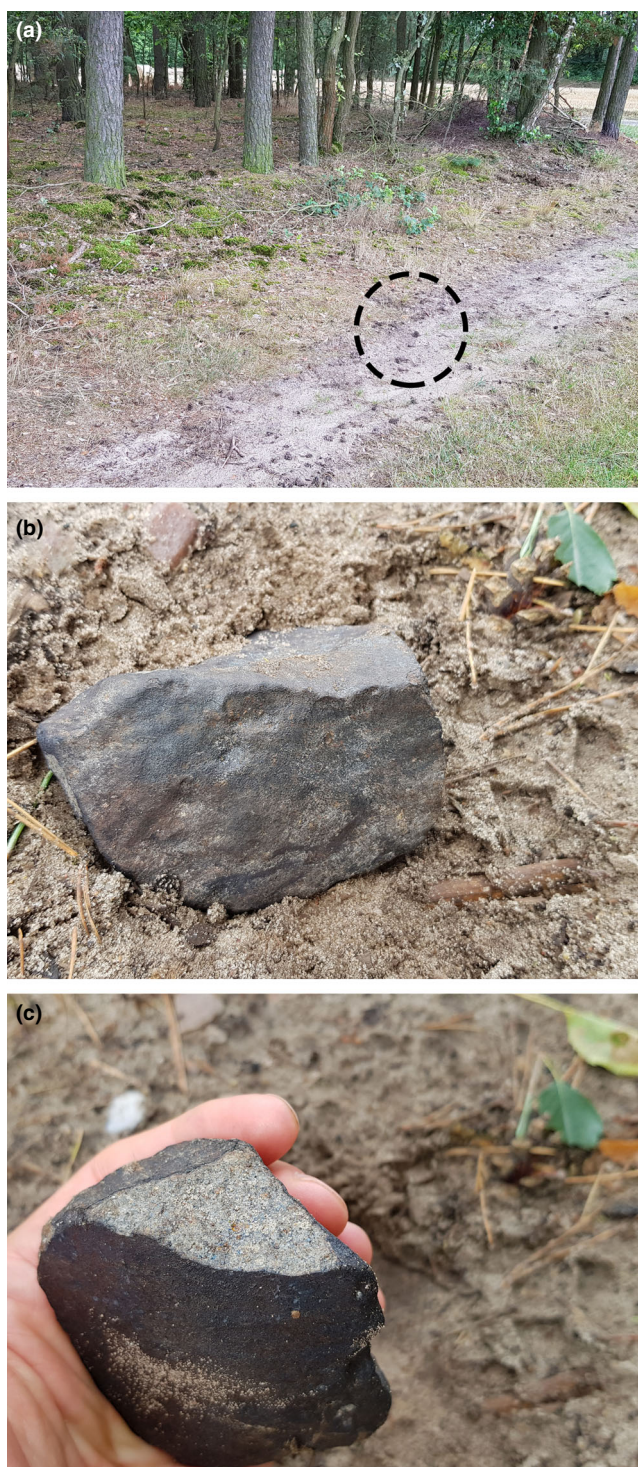


Fig. 4. a) The find site of the first discovered sample on a small dirt track at the border between farmland and forest. b) The sample at the impact site and (c) in hand—an amazing experience to be the first to touch this extraterrestrial stranger. (Color figure can be viewed at [wileyonlinelibrary.com](https://onlinelibrary.wiley.com/doi/10.1111/maps.15905).)

between 22.5 and 26.7 mole% Fa (Table 1). The low-Ca pyroxenes and Ca-pyroxenes have compositions of $\text{Fs}_{20.6 \pm 0.6} \text{Wo}_{1.2 \pm 0.6}$ and $\text{Fs}_{7.6 \pm 1.1} \text{Wo}_{43.5 \pm 3.4}$, respectively

(Table 2). The 96 analyzed low-Ca pyroxenes vary between 19.1 and 22.5 mole% Fs.

Large plagioclase grains ($>20 \mu\text{m}$) are rare, and plagioclase-rich areas are typically intergrown with mafic silicates. Typical plagioclase has An and Or components of 10.2 ± 2.3 and 4.5 ± 1.9 mole%, respectively ($n = 6$; Table 1), and the compositions vary between 7.5 and 13.9 mole% An. However, we also analyzed a single plagioclase with a higher An content (An_{25}). Both phosphates, namely merrillite and Cl-apatite, were found in the thin sections. The major element compositions of the two phosphates are also listed in Table 1. The apatite is rich in Cl (4.9 wt%) and is different from apatites in the recently analyzed Renchen L ordinary chondrite breccia, which have 3.4 wt% F (Bischoff, Barrat, et al., 2019). Such differences are completely unexpected for chondrites belonging to the same group as demonstrated by Ward et al. (2017).

Small grains of metals and sulfide occur throughout the entire thin sections. Their mean compositions are given in Table 2. However, large metallic phases are heterogeneously distributed. A metal-rich area (band) will be described below. In general, the metal grains of kamacite and taenite are heterogeneous in composition. Kamacite is by far most abundant. The Ni and Co concentrations of kamacite slightly vary (5.9–7.2 and 0.5–1.1 wt%, respectively). Also, the taenite composition is variable, with Ni content varying from 27 to 47 wt% and Co concentrations between 0.13 and 0.57 wt%.

The Metal-Rich Area

As shown in Figs. 1 and 5, a huge metal-rich band is observed in Antonin covering an area of roughly $3 \times 10 \text{ mm}$. Well-defined chondrules are completely enclosed in the metal (Fig. 7). In the optical microscope, this area looks very chondritic, resembling a type 4 lithology. This may be because metals surrounding the chondrules protected the chondrules from recrystallization during the period of thermal metamorphism. The dominant metal phase kamacite has a mean composition of 6.6 wt% Ni and 0.96 wt% Co. Only a few taenites were identified, which all occur at the border with the host silicates. The Ni concentration in kamacite from the metal-rich area is similar to that of kamacite in the bulk chondrite. However, the mean Co concentration is higher than in kamacite of the host meteorite. Notably, it is very homogeneous (0.86–1.1 wt%) compared to the metal grains outside this band in the bulk meteorite (0.57–1.1 wt%).

Shock Metamorphism and Weathering

Based on examinations of the two polished sections, Antonin is brecciated on a large scale (Figs. 1, 5, and 8)

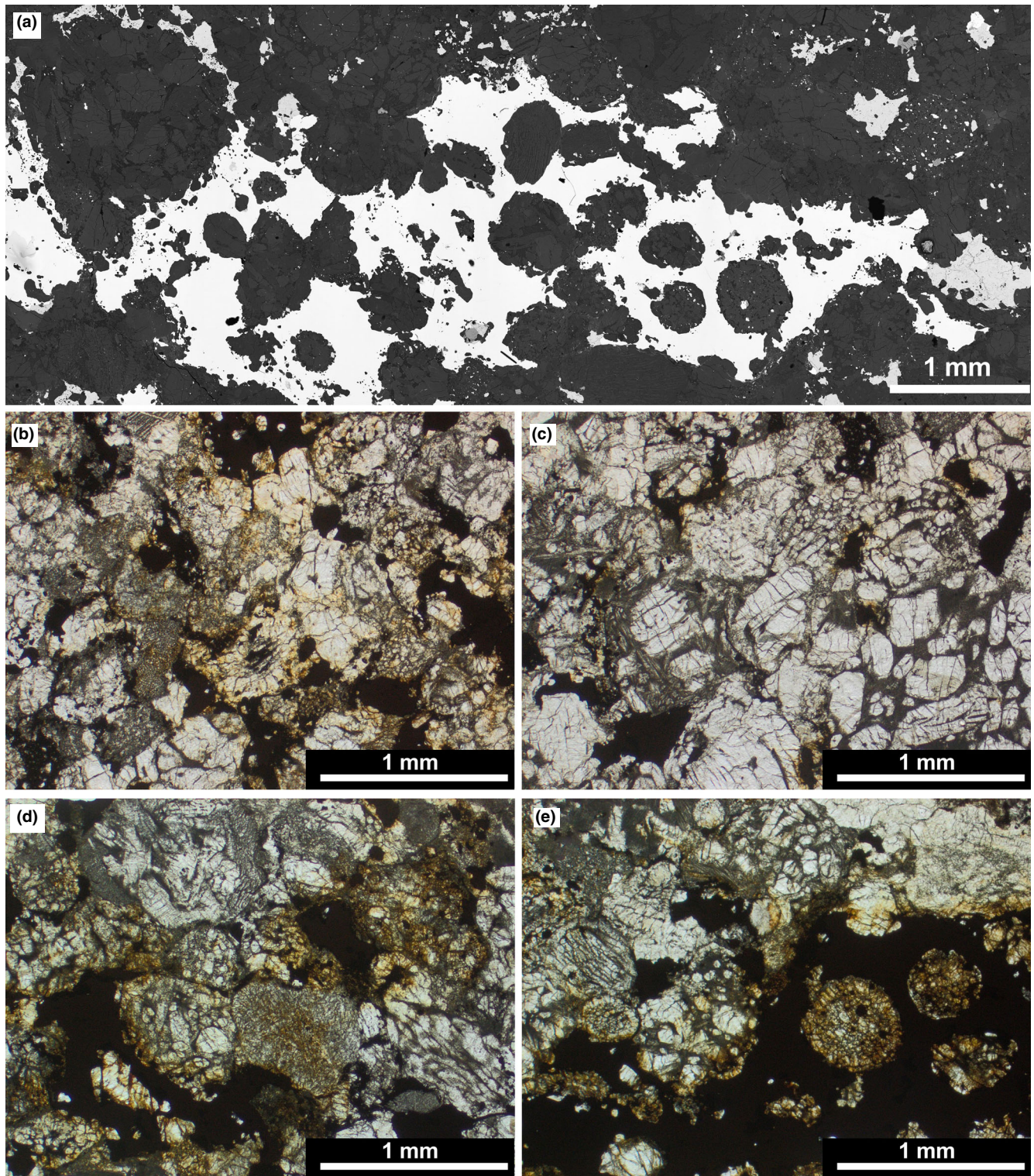


Fig. 5. a) The metal-rich area preserves a visible type 4 chondritic texture (backscattered electron image). b–e) Overview images of the two different lithologies in Antonin. The degree of recrystallization decreases from type 5 (b + c) to type 4/5 (d + e). Based on the abundant metal (opaque phase in [e]), individual chondrules are easily observed as in type 4 ordinary chondrites. Images (b)–(e) in plane polarized light. (Color figure can be viewed at wileyonlinelibrary.com.)

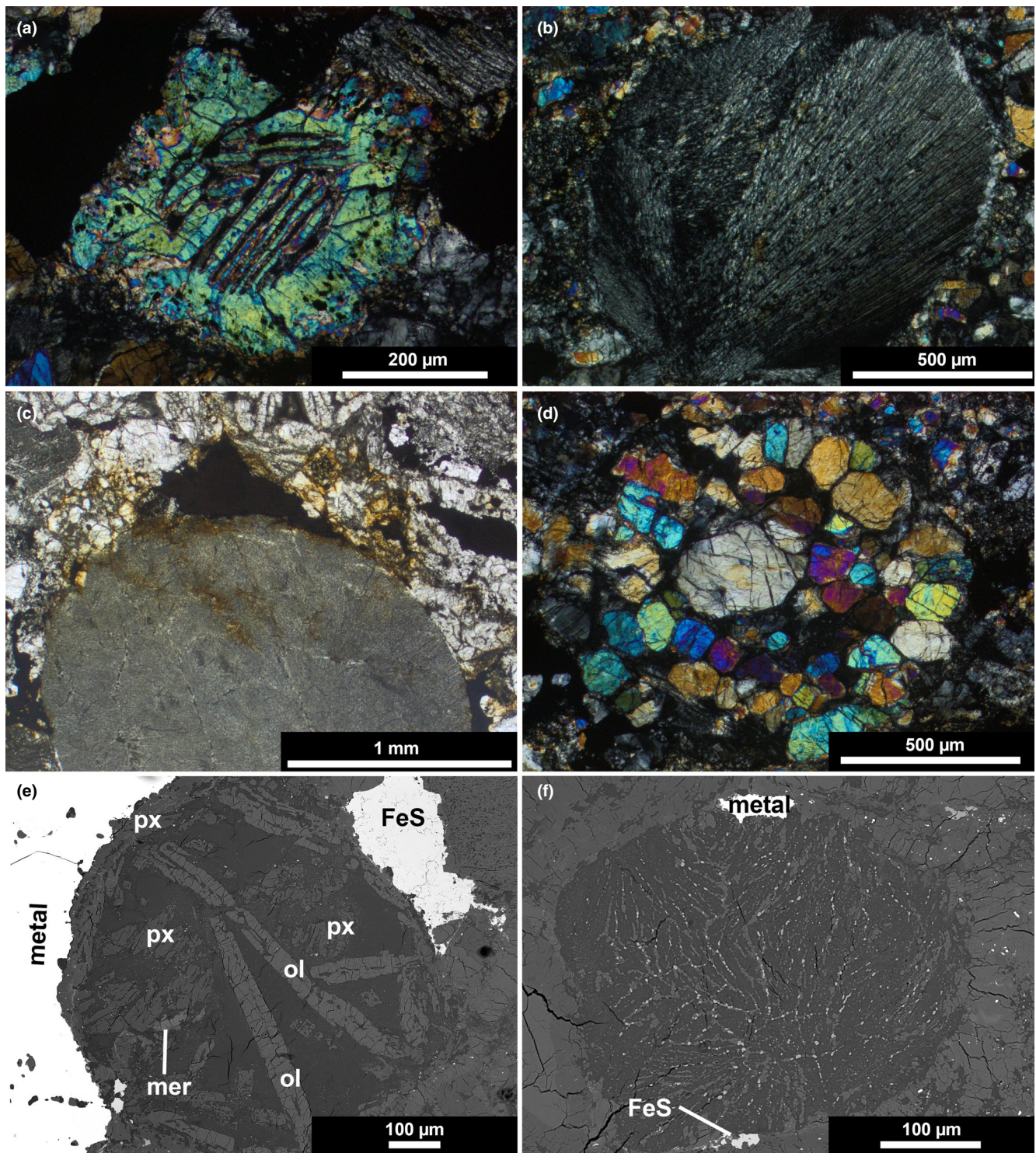


Fig. 6. Different types of chondrules in Antonin: (a) a barred olivine (BO) chondrule having a broad olivine rim; (b) radial pyroxene (RP) chondrule; (c) large cryptocrystalline (C) chondrule; (d) porphyritic olivine–pyroxene (POP) chondrule; (e) Na,Al-rich chondrule with olivine laths (ol), low-Ca pyroxene (px), and merrillite (mer) grains embedded a fine-grained, Na,Al-rich mesostasis, BSE image; (f) Na,Cr,Al-rich chondrule with abundant small chromite grains (light particles) and lath-like olivine (medium gray) enclosed in an Na-Al-rich groundmass, backscattered electron image. (Color figure can be viewed at wileyonlinelibrary.com.)

Table 1. Chemical composition of main phases in the Antonin breccia. All data in wt%; n.d. = not detected; n.a. = not analyzed; n = number of analyses; Px = pyroxene; Plag = plagioclase. * contains about 4.9 wt% Cl and 0.67 wt% F. ** not analyzed for Zn, V, etc., and not checked for Fe³⁺.

	Olivine <i>n</i> = 201	Px <i>n</i> = 96	Ca-Px <i>n</i> = 13	Plag <i>n</i> = 6	An ₂₅ Plag <i>n</i> = 1	Apatite <i>n</i> = 3	Merrillite <i>n</i> = 11	Chromite <i>n</i> = 6
SiO ₂	38.0	55.4	53.9	67.6	63.1	0.07	0.15	0.08
TiO ₂	<0.03	0.15	0.40	0.09	0.07	n.d.	n.d.	1.70
Al ₂ O ₃	<0.02	0.18	0.97	20.5	23.8	n.a.	n.a.	5.8
Cr ₂ O ₃	0.05	0.11	0.78	0.10	0.05	<0.02	<0.02	55.8
FeO	22.0	13.8	4.7	0.74	0.50	0.67	0.97	30.5
MnO	0.47	0.50	0.23	<0.03	0.05	n.d.	<0.02	0.78
MgO	39.2	29.4	17.0	0.18	0.06	<0.03	3.6	2.22
CaO	<0.03	0.62	21.0	2.08	5.0	53.2	46.2	<0.04
Na ₂ O	<0.02	0.05	0.71	9.7	7.7	0.45	2.62	<0.01
K ₂ O	<0.01	<0.01	<0.03	0.77	0.93	n.d.	<0.04	<0.01
P ₂ O ₅	n.d.	n.d.	n.d.	n.d.	n.d.	40.9	45.5	n.d.
Total	99.83	100.22	99.72	101.79	100.71	100.91*	99.12	96.94**
Fa	24.0 ± 0.5							
Fs		20.6 ± 0.6	7.6 ± 1.1					
Wo		1.2 ± 0.6	43.5 ± 3.4					
An				10.2 ± 2.3	25.1			
Or				4.5 ± 1.9	5.6			

Table 2. Chemical composition of metals and sulfide (troilite) in the Antonin breccia. The mean compositions are given for phases in the vein area (band; Fig. 5a) as well as for those from the host rock. All data in wt%; n.d. = not detected.

	Kamacite Bulk <i>n</i> = 15	Kamacite Vein area <i>n</i> = 18	Taenite Bulk <i>n</i> = 13	Taenite Vein area <i>n</i> = 5	Troilite Bulk <i>n</i> = 10	Troilite Vein area <i>n</i> = 7
Fe	93.4 ± 1.0	92.9 ± 1.1	64.6 ± 5.8	63.1 ± 8.5	63.1 ± 0.4	62.8 ± 0.3
Co	0.83 ± 0.15	0.96 ± 0.07	0.24 ± 0.06	0.31 ± 0.14	<0.05	<0.05
Ni	6.5 ± 0.22	6.6 ± 0.23	34.6 ± 5.7	36.1 ± 7.9	<0.03	<0.04
S	n.d.	n.d.	n.d.	n.d.	36.7 ± 0.2	36.4 ± 0.2
Total	100.73	100.46	99.44	99.51	99.88	99.29

and well lithified. Thus, the brecciation is difficult to see in thin section, because the so-far identified different lithic clasts show very similar degrees of recrystallization (petrologic types 4–5). Olivine grains show characteristic shock features in the form of weak mosaicism (Fig. 8), typical for a degree of shock metamorphism of S4 (Bischoff & Stöffler, 1992; Langenhorst et al., 2017; Stöffler et al., 1991, 2018). Besides the mosaicism, olivines also have well-developed planar fractures. Occasionally, small melt areas and veins were detected containing abundant small metal- and sulfide-rich spherules (Fig. 8d). High-pressure phases (such as ringwoodite) were not detected in the melt veins or at their borders. Such phases are often observed in L5 and L6 chondrites with a degree of shock metamorphism of S4 and also occur in a small number of LL chondrites (e.g., Bischoff, 2002; Bischoff, Schleiting, & Patzek, 2019; Hu & Sharp, 2022). Some feldspar glass or

maskelynite is restricted to the shock veins, but most feldspar certainly is crystalline. The shock stage (S4—moderately shocked) is the most abundant shock degree among the L chondrites (Bischoff, Schleiting, & Patzek, 2019).

The residence time of 18 days on the ground and the cutting of the sample with water resulted in initial signs of terrestrial weathering. The local presence of a brownish color results from the first breakdown of metals. Thus, a few rusty spots are especially recognizable with the naked eye on the surface of the samples and close to the metal-rich area (compare Figs. 1 and 4).

Chemical Characteristics

Bulk Chemistry

From a thin slice, 0.55 g was homogenized and 170 mg of the powder was provided for chemical

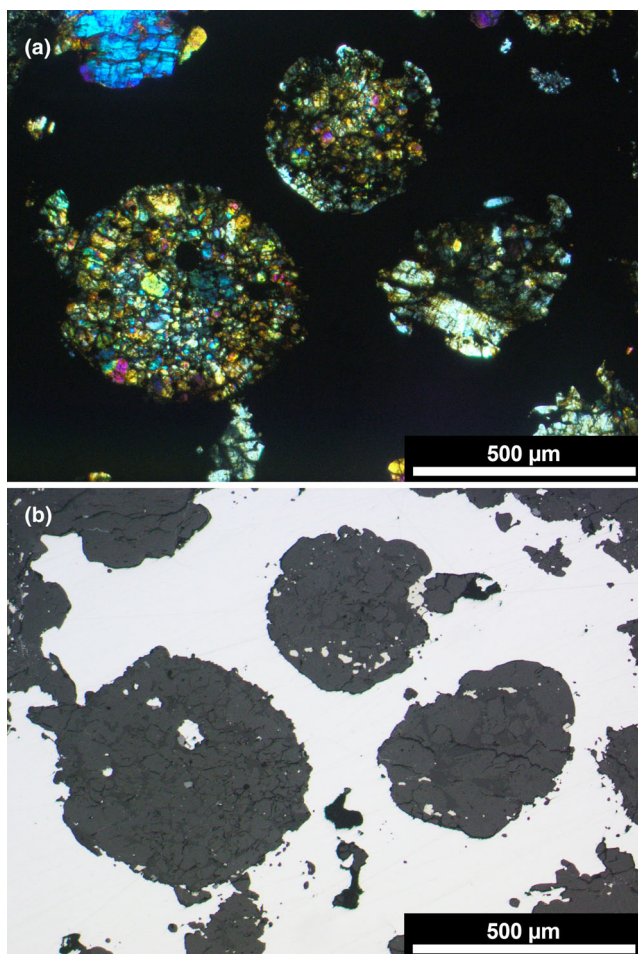


Fig. 7. Well-defined chondrules are visible within the metal-rich area. Microscopic images (a) in plane polarized light, crossed nicols; (b) in reflected light. (Color figure can be viewed at wileyonlinelibrary.com.)

characterization. The results are summarized in Table 3 and indicate that for most elements, the chemical composition of Antonin is close to the compositions of recently analyzed meteorite falls of Renchen, Braunschweig, and other L chondrites (Bartoschewitz et al., 2017; Bischoff, Barrat, et al., 2019; Lodders & Fegley, 1998). Thus, in general, the Antonin chondrite is indistinguishable from L chondrites. Considering some chalcophile elements (e.g., Cu, Zn, Ga), Mn, and the REE, a slight depletion (~10%) can be attested compared to those in average bulk L chondrites (Lodders & Fegley, 1998).

Oxygen Isotopes

The oxygen isotope compositions of the three analyzed fragments of Antonin are $\delta^{17}\text{O} = 3.42\text{‰}$, 3.58‰ , 3.50‰ ; and $\delta^{18}\text{O} = 4.65\text{‰}$, 4.75‰ , 4.70‰ , respectively. The mean $\Delta^{17}\text{O}$ of 1.02‰ , relative to a

reference line with a slope of 0.528, is similar to the compositions of other L chondrites, but is different from most other types of meteoritic materials (Fig. 9). The oxygen isotope data set, therefore, supports the classification of Antonin as an L chondrite.

Titanium Isotopes

The Ti isotopic composition of the Antonin whole-rock sample is $\epsilon^{50}\text{Ti} = -0.60 \pm 0.15$ ($n = 5$; Fig. 10). Within uncertainty, this composition is consistent with previous data of L chondrites (Trinquier et al., 2009; Zhang et al., 2012).

DISCUSSION

Mineralogical Properties and Classification of Antonin

Based on the presented results, Antonin is a breccia, but the brecciation is difficult to recognize (Figs. 1 and 8). Most individual fragments show recrystallized textures (types 4 and 5; Fig. 5) as indicated by recrystallized “relict” chondrules. These observations clearly point to a moderate metamorphic grade of the most abundant fragments within the Antonin chondrite. The medium-sized plagioclase grains (mostly $<20\ \mu\text{m}$) and the homogeneous compositions of olivine ($\text{Fa}_{24.0 \pm 0.5}$) and low-Ca pyroxene ($\text{Fs}_{20.6 \pm 0.6}$) also support this. Based on these mean compositions of olivine and low-Ca pyroxene, the rock clearly has to be classified as an L-group ordinary chondrite. The data are very similar to those reported by Shrubený et al. (2022), Krzesińska et al. (2022), and in The Meteorite Bulletin (2022). Antonin also contains areas with well-defined, only slightly recrystallized chondrules (Figs. 6 and 7). Since olivine and low-Ca pyroxene are also equilibrated, the petrologic type in these parts has to be defined as type 4 or type 4/5. Despite the high degree of chemical homogenization of olivine and pyroxene reported by Krzesińska et al. (2022), these authors also report that Antonin contains many chondrules and glassy mesostases that are retained in the sample. This would speak for some local type 3 components and would be consistent with the breccia classification made in this contribution. This may also would explain some differences in plagioclase compositions between the data reported here and within the Meteorite Bulletin Database (2022).

Thus, in summary, a classification of Antonin as an L4-5 breccia is most appropriate. However, as mentioned before, the brecciation is difficult to recognize, and Antonin does not belong to the meteorites with complex brecciation textures. The parent body was certainly less brecciated than asteroid 2008 TC₃ (which is the parent meteoroid of the Almahata Sitta stones) or the

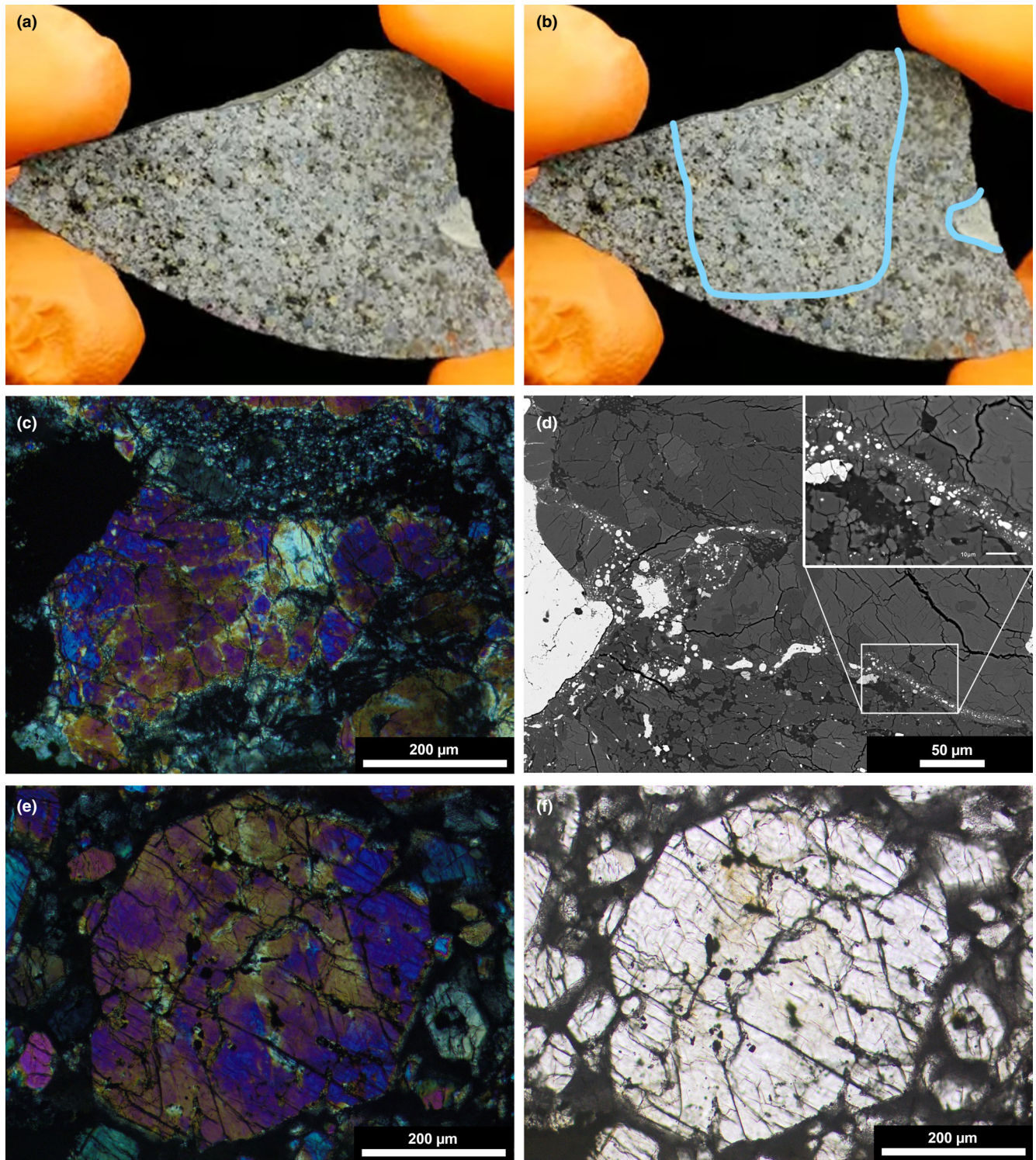


Fig. 8. Shock features in Antonin. a, b) The brecciated texture is visible and indicated in the hand specimen. c) A large olivine with distinct mosaicism (S4). d) Local area with a small melt pocket and vein containing small metal- and sulfide-rich spherules. e) Olivine with a low degree of mosaicism and planar fractures. f) Same object as in (e): Planar fractures with three different orientations are visible. (Color figure can be viewed at wileyonlinelibrary.com.)

Table 3. Trace and major element abundances of Antonin (bold values). (*) data in wt%, other data in ppm. Data for Braunschweig and Renchen are from Bartoschewitz et al. (2017) and Bischoff, Barrat, et al. (2019), respectively. The mean concentrations for the L chondrites are from Lodders and Fegley (1998).

Element	Renchen L5-6	Braunschweig L6	Antonin L4-5	Mean L chondrites
Al	1.01*	1.159*	1.01*	1.16*
Fe	21.5*	21.6*	22.0*	21.8*
Mg	16.65*	15.0*	14.4*	14.9*
Na	0.54*	0.712*	0.65*	0.69*
Ni	0.91*	1.23*	1.56*	1.24*
P	844	1310	905	1030
K	907	1021	873	920
Ca	1.33*	1.41*	1.21*	1.33
Sc	9.13	10.01	8.52	8.1
Ti	634	644	610	670
V	70.3	70.09	62.1	75
Cr	4372	3804	3048	3690
Mn	0.30*	0.267*	2478	2590
Co	518	601	582	580
Cu			84.6	90
Zn	29.9	43.96	42.4	57
Ga	4.11	5.05	4.81	5.4
Rb	2.73	3.06	2.59	2.8
Sr	10.68	11.34	10.5	11
Y	2.14	2.32	1.98	1.8
Zr	5.69	6.48	5.02	6.4
Nb	0.494	0.46	0.43	0.4
Cs	0.088	0.048	0.030	
Ba	4.17	3.78	3.53	4.1
La	0.317	0.328	0.277	0.318
Ce	0.816	0.873	0.711	0.970
Pr	0.162	0.128	0.107	0.140
Nd	0.757	0.649	0.538	0.700
Sm	0.195	0.218	0.176	0.303
Eu	0.0797	0.0827	0.079	0.080
Gd	0.262	0.30	0.243	0.317
Tb	0.0498	0.0549	0.045	0.059
Dy	0.337	0.378	0.306	0.372
Ho	0.0754	0.0835	0.069	0.089
Er	0.225	0.250	0.302	0.252
Tm			0.031	0.038
Yb	0.230	0.256	0.206	0.226
Lu	0.0354	0.0392	0.0313	0.034
Hf	0.173	0.197	0.152	0.170
Ta	0.0253	0.0227	0.0216	0.021
Pb	0.0658	0.0336	0.0316	0.040
Th	0.0650	0.0452	0.034	0.042
U	0.0291	0.0128	0.0102	0.015

parent body of Kaidun, which both include a great number of clasts or stones of different meteorite classes and types (e.g., Bischoff et al., 2010; Bischoff, Bannemann, et al., 2022; Goodrich et al., 2014;

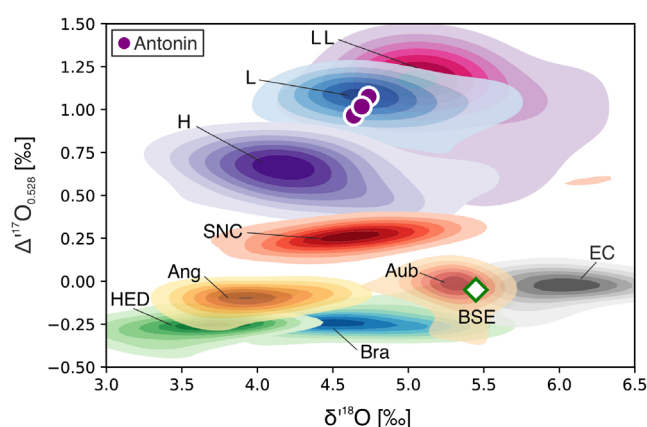


Fig. 9. Triple oxygen isotope compositions ($\Delta^{17}\text{O}$ versus $\delta^{18}\text{O}$) of three individual chips (~2 mg each) of Antonin, compared to the compositions of ordinary chondrites (H, L, LL) and other stony meteorite groups from the noncarbonaceous clan (EC = enstatite chondrites; HED = howardites, eucrites, diogenites; Aub = aubrites, Ang = angrites, Bra = brachinites; SNC = shergottites, nakhlites, chassignites) and the bulk silicate Earth (BSE). Meteorite reference compositions were compiled from the Meteoritical Bulletin Database and are shown with Kernel density estimation contours, with the outermost contours for a given meteorite group encompassing 70% of the corresponding data populations. The composition of the bulk silicate Earth (BSE) was taken from Peters et al. (2021). (Color figure can be viewed at wileyonlinelibrary.com.)

Horstmann et al., 2010; Horstmann & Bischoff, 2014; Zolensky et al., 1996, 2010; Zolensky & Ivanov, 2003). It was also less brecciated than the parent bodies of other complex breccias among the ordinary chondrites, which also contain different rock types (e.g., Bischoff et al., 1993, 2006, 2018; Bischoff, Dyl, et al., 2013; Bischoff, Horstmann, et al., 2013; Metzler et al., 2010, 2011; Rubin et al., 2005, 2017).

Considering the onion shell model for the setting of the parent body, no unequilibrated clasts that may originate from the near surface areas (type 3) of the Antonin parent body were mixed into this breccia during impact-induced lithification (Bischoff et al., 1983; Kieffer, 1975). However, the large metal-rich areas visible (Fig. 5) may represent a specific lithology that will be discussed in detail below.

Besides the fragments of type 4 to type 5, the occurrence of small impact melt areas and thin impact melt veins and pockets are clearly visible (Fig. 8). Based on the weak mosaicism in olivine within the entire rock, the chondrite is moderately shocked (S4). Thus, Antonin is an L4-5, S4 ordinary chondrite breccia.

Chemical Properties of Antonin

The L chondrite classification is confirmed by the bulk chemical data (Table 3) as well as the results of the

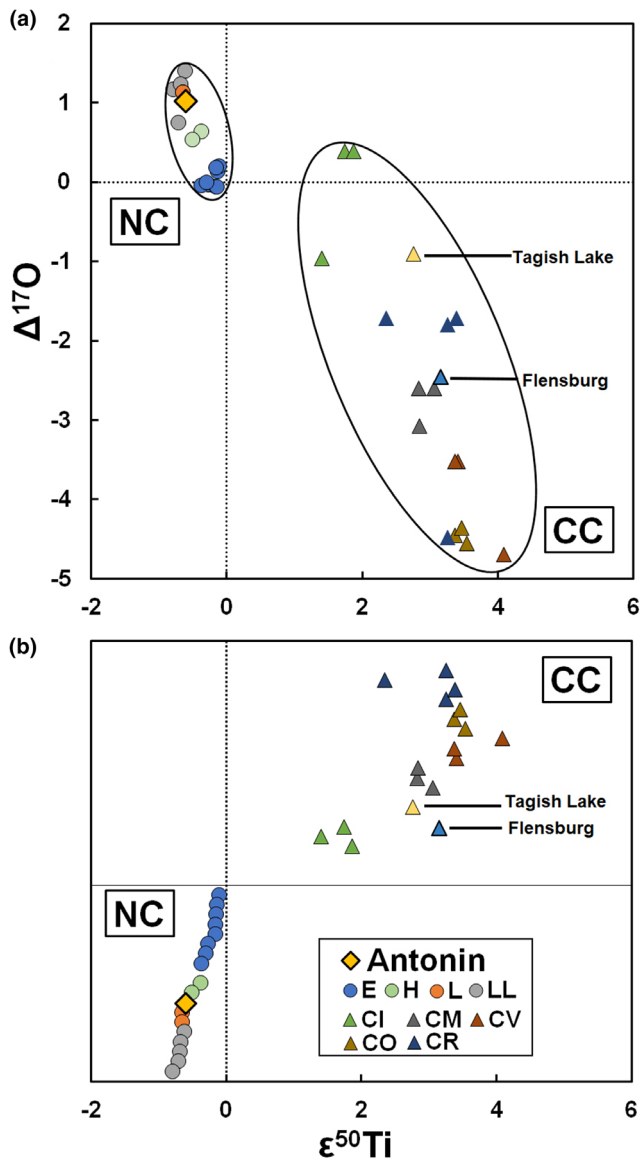


Fig. 10. The $\epsilon^{50}\text{Ti}$ values (a,b) in noncarbonaceous (NC) and carbonaceous chondrites (CC) as well as correlated with $\Delta^{17}\text{O}$ data (a). Antonin clearly belongs to the noncarbonaceous meteorites. The error for Antonin is within the size of the symbol. Data from Clayton et al. (1991), Clayton and Mayeda (1996, 1999), Newton et al. (2000), Greenwood and Franchi (2004), Leya et al. (2008), Trinquier et al. (2009), Greenwood et al. (2010), Schrader et al. (2011), Zhang et al. (2011, 2012), Gerber et al. (2017), Bischoff et al. (2017, 2021), and Bischoff, Barrat, et al. (2019). (Color figure can be viewed at [wileyonlinelibrary.com](https://onlinelibrary.wiley.com).)

analyses of the O and Ti isotopes (Figs. 9 and 10). Considering the REE, the Antonin chondrite displays a slight negative Tm anomaly that is typical to other OC and typical of inner solar system materials (e.g., Barrat et al., 2016). As stated in the Results section, some chalcophile elements (e.g., Cu, Zn, Ga) and other

elements (e.g., REE) are slightly depleted (~10%) compared to those in average bulk L chondrites (Lodders & Fegley, 1998). This effect can be related to the inhomogeneous distribution of various components in the bulk sample. It is certainly not related to the occurrence of the metal–chondrule aggregate as shown in Fig. 5a (see also below), since the analyzed aliquot of the sample is not depleted in the siderophile elements Fe, Co, and Ni. Since we already detected the completely (for chondrites) untypical metal–chondrule assemblage, other chemical features (depletions of chalcophile elements, REE, etc.) may also show a heterogeneous distribution in the Antonin breccia. We have no explanation for this observation. Effects of terrestrial alteration as found in meteorite finds (e.g., Stelzner et al., 1999) can be ruled out.

The Metal-Rich Area and the Heterogeneous Distribution of Metal in Antonin

From the various images taken of the rock, peculiar areas are visible consisting of large, eye-catching metal–silicate assemblages. This is also the case in one of our thin sections and is shown in Figs. 5 and 7. This metal has an extremely homogeneous composition, especially considering the Co and Ni concentrations, whereby it can be basically characterized as kamacite enclosing perfectly round-shaped chondrules (Fig. 7). Well-defined chondrules also occur at the edges of the kamacite areas. This chondrule–kamacite assemblage can arise by different processes in its early evolution. Since the well-defined chondrules are completely enclosed in metal, the chondrule formation must clearly precede the formation of the assemblage. The following possibilities exist:

- Metal–chondrule aggregation by metal condensation onto chondrules in the nebula;
- Metal–chondrule aggregate formation by chondrule incorporation due to nebular collisions of chondrules with large molten metal droplets;
- Formation of the metal–chondrule assemblage by impact-induced local metal mobilization and incorporation of chondrules on the meteorite parent body.

Considering these possibilities, we cannot offer an unambiguous explanation for the formation of this kind of metal–chondrule assemblage. Also, we cannot completely rule out one of the above-listed possible processes of formation. However, since the chondrules are intact, well preserved, and not strongly recrystallized, we can rule out that they were incorporated into the metal during the brecciation event or at the impact process that triggered the mosaicism of olivine (S4).

The Most Recent and Most Important Polish Meteorites

Before Antonin, the most recent confirmed meteorite falls in Poland were registered in 2011 (Soltmany, L6 ordinary chondrite), 1995 (Baszkowka, L5 ordinary chondrite), and 1935 (Lowicz, mesosiderite). These data from the Meteoritical Bulletin clearly demonstrate that recovering a meteorite fall in Poland is rare, likely because of its lush vegetation in most regions and its abundance of sparsely populated areas. The meteorite Pultusk (H5), an 1868 fall with a total mass of about 250 kg that produced a huge strewn field, is one of the most studied meteorites from Poland (e.g., Chen & Wasserburg, 1980; Ganapathy & Anders, 1973; Krzesińska et al., 2015; Lang & Kowalski, 1971; Stöffler et al., 1991). Another well-known, well-studied fall is the polymict eucrite Białystok (e.g., Delaney et al., 1983; Metzler & Stöffler, 1987). Among the finds, prominent and well-studied Polish samples include those of the Morasko meteorite, a 290 kg iron meteorite—with the largest mass among the Polish samples—and the ungrouped enstatite meteorite Zakłodzie (e.g., Buchwald, 1975; Kracher et al., 1980; Krzesińska et al., 2019; Patzer et al., 2002; Przylibski et al., 2005; Slavik & Spencer, 1928; Stepniowski et al., 2000).

The Antonin Meteorite and the Fall Statistics in Central Europe

Since 2013, 10 meteorite falls have been recovered in an area less than 500 km in radius. All are ordinary chondrites except Flensburg, which is a small spectacular C1 chondrite (Bischoff et al., 2021). Considering the other meteorite falls of Braunschweig (L6; Bartoschewitz et al., 2017), Žďár nad Sázavou (L3; Kalasová et al., 2020; Spurný, 2016; Spurný et al., 2016; Spurný et al., 2020), Ejby (H5/6; Spurný et al., 2017; Haack et al., 2019), Stubenberg (LL6; Bischoff et al., 2017; Ebert & Bischoff, 2016b; Spurný et al., 2016), Hradec Králové (LL5; 2016; The Meteoritical Bulletin), Broek in Waterland (L6, 2017; The Meteoritical Bulletin), Renchen (L5-6; Bischoff, Barrat, et al., 2019), and Kindberg (L6, 2020; The Meteoritical Bulletin), Antonin is the ninth recovered ordinary chondrite fall since 2013. In the same time, at least three other chondritic finds were recognized alone in Germany (Blaubeuren, Cloppenburg, and Machtenstein; Bischoff, Storz, et al., 2022). Considering these data, it is obvious that the number of meteorite falls in Central Europe is remarkable and certainly related to the successful work of the European Fireball Network and the great initiatives of the International Meteor Organization (IMO) and the American Meteor Society (AMS). The success of these organizations directly relates to the

excellent recorded fireball events and the calculations of possible meteorite strewn fields.

CONCLUSIONS

In the early morning of July 15, 2021, the meteorite of Antonin fell about 20 km south of Ostrowo (Poland). So far, only one fragment of 350 g was discovered August 3, 2021, already 18 days after the fireball event based on the exact calculations of the possible strewn field.

Based on mean compositions of equilibrated olivine and low-Ca pyroxene grains as well as on the O isotope characteristics, Ti isotopes, and bulk chemistry, the rock is classified as an L-group ordinary chondrite. The weak mosaicism of olivine indicates a shock degree of S4. Based on the brecciated features, an exact classification of L4-5 (S4) is appropriate.

The inspection of the hand specimen and, especially, of the studied subsample indicates that the metal in Antonin is heterogeneously distributed.

Acknowledgments—We thank Ulla Heitmann for technical assistance and Celeste Brennecke for editorial support. We acknowledge the helpful reviews of Alan Rubin and an anonymous reviewer and thank the Associate Editor Mike Zolensky. This work is partly funded by the Deutsche Forschungsgemeinschaft (DFG, German Research Foundation)—Project-ID 263649064—TRR 170 (A.B.) and Project-ID 463342295 (S.E.). This is TRR170 Publication No. 163. M.P. is partly funded by a Sofja Kovalevskaja Award of the Alexander von Humboldt Foundation. Open Access funding enabled and organized by Projekt DEAL.

Data Availability Statement—Data available on request from the authors.

Editorial Handling—Dr. Michael Zolensky

REFERENCES

- Barrat, J.-A., Gillet, P., Dauphas, N., Bollinger, C., Etoubleau, J., Bischoff, A., and Yamaguchi, A. 2016. Evidence from tm Anomalies for Non-CI Refractory Lithophile Element Proportions in Terrestrial Planets and Achondrites. *Geochimica et Cosmochimica Acta* 176: 1–17.
- Barrat, J.-A., Rouxel, O., Wang, K., Moynier, F., Yamaguchi, A., Bischoff, A., and Langlade, J. 2015. Early Stages of Core Segregation Recorded by Fe Isotopes in an Asteroidal Mantle. *Earth and Planetary Science Letters* 419: 93–100.
- Barrat, J.-A., Zanda, B., Moynier, F., Bollinger, C., Liorzou, C., and Bayron, G. 2012. Geochemistry of CI Chondrites: Major and Trace Elements, and Cu and Zn Isotopes. *Geochimica et Cosmochimica Acta* 83: 79–92.

- Bartoschewitz, R., Appel, P., Barrat, J.-A., Bischoff, A., Caffee, M. W., Franchi, I. A., Gabelica, Z., et al. 2017. The Braunschweig Meteorite—A Recent L6 Chondrite Fall in Germany. *Chemie der Erde Geochemistry* 77: 207–24.
- Bischoff, A. 2002. Discovery of Purple-Blue Ringwoodite within Shock Veins of an LL6 Ordinary Chondrite from Northwest Africa (Abstract #1264). 33rd Lunar and Planetary Science Conference. CD-ROM.
- Bischoff, A., Alexander, C. M. O'D., Barrat, J.-A., Burkhardt, C., Busemann, H., Degering, D., Di Rocco, T., et al. 2021. The Old, Unique C1 Chondrite Flensburg—Insight into the First Processes of Aqueous Alteration, Brecciation, and the Diversity of Water-Bearing Parent Bodies and Lithologies. *Geochimica et Cosmochimica Acta*. 293: 142–86.
- Bischoff, A., Bannemann, L., Decker, S., Ebert, S., Haberer, S., Heitmann, U., Horstmann, M., et al. 2022. Asteroid 2008 TC₃, Not a Polymict Ureilitic but a Polymict C1 Chondrite Parent Body?—Survey of 249 Almahata Sitta Fragments. *Meteoritics & Planetary Science* 57: 1339–64.
- Bischoff, A., Barrat, J.-A., Bauer, K., Burkhardt, C., Busemann, H., Ebert, S., Gonsior, M., et al. 2017. The Stubenberg Meteorite—An LL6 Chondrite Fragmental Breccia Recovered Soon after Precise Prediction of the Strewn Field. *Meteoritics & Planetary Science* 52: 1683–703.
- Bischoff, A., Barrat, J.-A., Berndt, J., Borovička, J., Burkhardt, C., Busemann, H., Hakenmüller, J., et al. 2019. The Renchen L5-6 Chondrite Breccia—The First Confirmed Meteorite Fall from Baden-Württemberg (Germany). *Geochemistry* 79: 125525.
- Bischoff, A., Dyl, K. A., Horstmann, M., Ziegler, K., Wimmer, K., and Young, E. D. 2013. Reclassification of Villalbeta de la Peña—Occurrence of a Winonaite-Related Fragment in a Hydrothermally Metamorphosed Polymict L-Chondritic Breccias. *Meteoritics & Planetary Science* 48: 628–40.
- Bischoff, A., Geiger, T., Palme, H., Spettel, B., Schultz, L., Scherer, P., Schlüter, J., and Lkhamsuren, J. 1993. Mineralogy, Chemistry, and Noble Gas Contents of Adzhi-Bogdo – An LL3-6 Chondritic Breccia with L-Chondritic and Granitoid Clasts. *Meteoritics* 28: 570–8.
- Bischoff, A., Horstmann, M., Pack, A., Laubenstein, M., and Haberer, S. 2010. Asteroid 2008 TC₃ – Almahata Sitta: A Spectacular Breccia Containing Many Different Ureilitic and Chondritic Lithologies. *Meteoritics & Planetary Science* 45: 1638–56.
- Bischoff, A., Horstmann, M., Vollmer, C., Heitmann, U., and Decker, S. 2013. Chelyabinsk—Not Only another Ordinary LL5 Chondrite, but a Spectacular Chondrite Breccia (Abstract #5171). *Meteoritics & Planetary Science* 48: A61.
- Bischoff, A., and Keil, K. 1983a. Ca-Al-Rich Chondrules and Inclusions in Ordinary Chondrites. *Nature* 303: 588–92.
- Bischoff, A., and Keil, K. 1983b. Catalog of Al-Rich Chondrules, Inclusions and Fragments in Ordinary Chondrites. Special Publication No. 22, UNM, Institute of Meteoritics, Albuquerque, 1–33.
- Bischoff, A., and Keil, K. 1984. Al-Rich Objects in Ordinary Chondrites: Related Origin of Carbonaceous and Ordinary Chondrites and their Constituents. *Geochimica et Cosmochimica Acta* 48: 693–709.
- Bischoff, A., Rubin, A. E., Keil, K., and Stöffler, D. 1983. Lithification of Gas-Rich Chondrite Regolith Breccias by Grain Boundary and Localized Shock Melting. *Earth and Planetary Science Letters* 66: 1–10.
- Bischoff, A., Schleiting, M., and Patzek, M. 2019. Shock Stage Distribution of 2280 Ordinary Chondrites—Can Bulk Chondrites with a Shock Stage S6 Exist as Individual Rocks? *Meteoritics & Planetary Science* 54: 2189–202.
- Bischoff, A., Schleiting, M., Wieler, R., and Patzek, M. 2018. Brecciation among 2280 Ordinary Chondrites—Constraints on the Evolution of Their Parent Bodies. *Geochimica et Cosmochimica Acta* 238: 516–41.
- Bischoff, A., Scott, E. R. D., Metzler, K., and Goodrich, C. A. 2006. Nature and Origins of Meteoritic Breccias. In *Meteorites and the Early Solar System II*, edited by D. S. Lauretta and H. Y. McSween, Jr., 679–712. Tucson, Arizona: University of Arizona.
- Bischoff, A., and Stöffler, D. 1992. Shock Metamorphism as a Fundamental Process in the Evolution of Planetary Bodies: Information from Meteorites. *European Journal of Mineralogy* 4: 707–55.
- Bischoff, A., Storz, J., Barrat, J.-A., Heinlein, D., Jull, A. J. T., Merchel, S., Pack, A., and Rugel, G. 2022. Blaubeuren, Cloppenburg, and Machtenstein—Three Recently Recognized H-Group Chondrite Finds in Germany with Distinct Terrestrial Ages and Weathering Effects. *Meteoritics & Planetary Science* 57: 136–53.
- Buchwald, V. F. 1975. *Handbook of Iron Meteorites*, vol. 3. Berkeley: University of California Press.
- Burkhardt, C., Dauphas, N., Hans, U., Bourdon, B., and Kleine, T. 2019. Elemental and Isotopic Variability in Solar System Materials by Mixing and Processing of Primordial Disk Reservoirs. *Geochimica et Cosmochimica Acta* 261: 145–70.
- Chen, J. H., and Wasserburg, G. J. 1980. A Search for Isotopic Anomalies in Uranium. *Geophysical Research Letters* 7: 275–8.
- Clayton, R. N., and Mayeda, T. K. 1996. Oxygen Isotope Studies of Achondrites. *Geochimica et Cosmochimica Acta* 60: 1999–2017.
- Clayton, R. N., and Mayeda, T. K. 1999. Oxygen Isotope Studies of Carbonaceous Chondrites. *Geochimica et Cosmochimica Acta* 63: 2089–104.
- Clayton, R. N., Mayeda, T. K., Goswami, J. N., and Olsen, E. J. 1991. Oxygen Isotope Studies of Ordinary Chondrites. *Geochimica et Cosmochimica Acta* 55: 2317–37.
- Clayton, R. N., Onuma, N., and Mayeda, T. K. 1976. A Classification of Meteorites Based on Oxygen Isotopes. *Earth and Planetary Science Letters* 30: 10–8.
- Delaney, J. S., Takeda, H., Prinz, M., Nehru, C. E., and Harlow, G. E. 1983. The Nomenclature of Polymict Basaltic Achondrites. *Meteoritics* 18: 103–11.
- Ebert, S., and Bischoff, A. 2016a. Genetic Relationship between Na-Rich Chondrules and Ca,Al-Rich Inclusions? – Formation of Na-Rich Chondrules by Melting of Refractory and Volatile Precursors in the Solar Nebula. *Geochimica et Cosmochimica Acta* 177: 182–204.
- Ebert S., and Bischoff A. 2016b. The Stubenberg (Bavaria) Ordinary Chondrite Breccia: The Latest German Meteorite Fall (Abstract #6137). *Meteoritics & Planetary Science* 51.
- Ebert, S., Render, J., Brennecka, G. A., Burkhardt, C., Bischoff, A., Gerber, S., and Kleine, T. 2018. Ti Isotopic Evidence for a Non-CAI Refractory Component in the

- Inner Solar System. *Earth and Planetary Science Letters* 498: 257–65.
- Ganapathy, R., and Anders, E. 1973. Noble Gases in Eleven H-Chondrites. *Geochimica et Cosmochimica Acta* 37: 359–62.
- Gerber, S., Burkhardt, C., Budde, G., Metzler, K., and Kleine, T. 2017. Mixing and Transport of Dust in the Early Solar Nebula as Inferred from Titanium Isotope Variations among Chondrules. *The Astrophysical Journal Letters* 841: L17.
- Goodrich, C. A., Bischoff, A., and O'Brien, D. P. 2014. Asteroid 2008 TC₃ and the Fall of Almahata Sitta, a Unique Meteorite Breccia. *Elements* 10: 31–7.
- Greenwood, R. C., and Franchi, I. A. 2004. Alteration and Metamorphism of CO₃ Chondrites: Evidence from Oxygen and Carbon Isotopes. *Meteoritics and Planetary Science* 39: 1823–38.
- Greenwood, R. C., Franchi, I. A., Kearsley, A. T., and Alard, O. 2010. The Relationship between CK and CV Chondrites. *Geochimica et Cosmochimica Acta* 74: 1684–705.
- Haack, H., Sørensen, A. N., Bischoff, A., Patzek, M., Barrat, J.-A., Midtskoge, S., Stempel, E., et al. 2019. Ejby—A New H5/6 Ordinary Chondrite Fall in Copenhagen, Denmark. *Meteoritics & Planetary Science* 54: 1853–69.
- Herwartz, D., Pack, A., Friedrichs, B., and Bischoff, A. 2014. Identification of the Giant Impactor Theia in Lunar Rocks. *Science* 344: 1146–50.
- Horstmann, M., and Bischoff, A. 2014. The Almahata Sitta Polymict Breccia and the Late Accretion of Asteroid 2008 TC₃—Invited Review. *Chemie der Erde – Geochemistry* 74: 149–84.
- Horstmann, M., Bischoff, A., Pack, A., and Laubenstein, M. 2010. Almahata Sitta—Fragment MS-CH: Characterization of a New Chondrite Type. *Meteoritics & Planetary Science* 45: 1657–67.
- Hu, J., and Sharp, T. G. 2022. Formation, Preservation and Extinction of High-Pressure Minerals in Meteorites: Temperature Effects in Shock Metamorphism and Shock Classification. *Progress in Earth and Planetary Science* 9: 6.
- Kalasová, D., Zikmund, T., Spurný, P., Haloda, J., Borovička, J., and Kaiser, R. J. 2020. Chemical and Physical Properties of Z⁶ar nad Sazavou L Chondrite and Porosity Differentiation using Computed Tomography. *Meteoritics & Planetary Science* 55: 1073–81.
- Kieffer, S. W. 1975. From Regolith to Rock by Shock. *The Moon* 13: 301–20.
- Kracher, A., Willis, J., and Wasson, J. T. 1980. Chemical Classification of Iron Meteorites-IX. A New Group (IIF), Revision of IAB and IIICD, and Data on 57 Additional Irons. *Geochimica et Cosmochimica Acta* 44: 773–87.
- Krzesińska, A., Gattacceca, J., Friedrich, J. M., and Rochette, P. 2015. Impact-Related Noncoaxial Deformation in the Pułtusk H Chondrite Inferred from Petrofabric Analysis. *Meteoritics & Planetary Science* 50: 401–17.
- Krzesińska A. M., Tymiński Z., Kmiecik K., Shrbený L., Spurný P. J., and Borovička J. 2022. The Antonin L5 Chondrite Fall (Poland): Mineralogy and Petrology of Meteorite, Bolide Trajectory and Meteoroid Orbit (Abstract #6144). 85th Annual Meeting of the Meteoritical Society.
- Krzesińska, A. M., Wirth, R., and Kusiak, M. A. 2019. Petrogenesis of Ungrouped Enstatite Meteorite Zakłodzie: Fabric, Texture, and Nanostructure Analysis for Identification of Mechanisms Responsible for Chondrite–Achondrite Transition. *Meteoritics & Planetary Science* 54: 1462–77.
- Lang, B., and Kowalski, M. 1971. On the Possible Number and Mass of Fragments from Pultusk Meteorite Shower, 1868. *Meteoritics* 6: 149–58.
- Langenhorst, M. C., Iancu, V., Tarcea, N., Langenhorst, F., Popp, J., 2017. Raman Spectroscopy of Experimentally Shocked Oligoclase (Abstract #1574). 48th Lunar and Planetary Science Conference. CD-ROM.
- Leya, I., Schönbächler, M., Wiechert, U., Krähenbühl, U., and Halliday, A. N. 2008. Titanium Isotopes and the Radial Heterogeneity of the Solar System. *Earth and Planetary Science Letters* 266: 233–44.
- Lodders K., and Fegley B. Jr. 1998. *The Planetary Scientist's Companion*. New York: Oxford University Press. p. 371.
- Metzler, K., Bischoff, A., Greenwood, R. C., Palme, H., Gellissen, M., Hopp, J., Franchi, I. A., and Trieloff, M. 2011. The L3-6 Chondritic Regolith Breccia Northwest Africa (NWA) 869: (I) Petrology, Chemistry, Oxygen Isotopes, and Ar-Ar Age Determinations. *Meteoritics & Planetary Science* 46: 652–80.
- Metzler, K., Bischoff, A., Palme, H., and Gellissen, M. 2010. Impact Melt Rocks from the L3-6 Chondritic Regolith Breccia Northwest Africa (NWA) 869. *Meteoritics & Planetary Science* 45: A137.
- Metzler, K., and Stöffler, D. 1987. Polymict Impact Breccias on the Eucrite Parent Body: I. Lithic Clasts in some Eucrites and Howardites (Abstract). In *Lunar and Planetary Science XVIII*, 641–2. Houston: Lunar and Planetary Institute.
- Millet, M.-A., and Dauphas, N. 2014. Ultra-Precise Titanium Stable Isotope Measurements by Double-Spike High Resolution MC-ICP-MS. *Journal of Analytical Atomic Spectrometry* 29: 1444–58.
- Newton, J., Franchi, I. A., and Pillinger, C. T. 2000. The Oxygen-Isotopic Record in Enstatite Meteorites. *Meteoritics and Planetary Science* 35: 689–98.
- Niederer, F., Papanastassiou, D., and Wasserburg, G. 1981. The Isotopic Composition of Titanium in the Allende and Leoville Meteorites. *Geochimica et Cosmochimica Acta* 45: 1017–31.
- Pack, A., and Herwartz, D. 2014. The Triple Oxygen Isotope Composition of the Earth Mantle and Understanding $\Delta^{17}\text{O}$ Variations in Terrestrial Rocks and Minerals. *Earth and Planetary Science Letters* 390: 138–45.
- Pack, A., Höweling, A., Hezel, D. C., Stefanak, M., Beck, A. K., Peters, S. T. M., Sengupta, S., Herwartz, D., and Folco, L. 2017. Tracing the Oxygen Isotope Composition of the Upper Earth Atmosphere Using Cosmic Spherules. *Nature Communications* 8: 15702.
- Pack, A., Tanaka, R., Hering, M., Sengupta, S., Peters, S., and Nakamura, E. 2016. The Oxygen Isotope Composition of San Carlos Olivine on VSMOW2-SLAP2 Scale. *Rapid Communications in Mass Spectrometry* 30: 1495–504.
- Patzer, A., Hill, D. H., Boynton, W. V., Franke, L., Schultz, L., Jull, A. J. T., McHargue, L. R., and Franchi, I. A. 2002. Itqiy: A Study of Noble Gases and Oxygen Isotopes Including its Terrestrial Age and a Comparison with Zakłodzie. *Meteoritics & Planetary Science* 37: 823–33.
- Peters, S. T. M., Alibabae, N., Pack, A., McKibbin, S. J., Raeisi, D., Nayebi, N., Torab, F., Ireland, T., and Lehmann, B. 2020. Triple Oxygen Isotope Variations in Magnetite from Iron-Oxide Deposits, Central Iran, Record Magmatic Fluid Interaction with Evaporite and Carbonate Host Rocks. *Geology* 48: 211–5.

- Peters, S. T. M., Fischer, M. B., Pack, A., Szilas, K., Appel, P. W. U., Muenker, C., Dallai, L., and Marien, C. S. 2021. Tight Bounds on Missing Late Veneer in Early Archean Peridotite from Triple Oxygen Isotopes. *Geochemical Perspectives Letters* 18: 27–31.
- Przylibski, T. A., Zagodzón, P. P., Kryza, R., and Pilski, A. S. 2005. The Zakłodzie Enstatite Meteorite: Mineralogy, Petrology, Origin, and Classification. *Meteoritics & Planetary Science* 40: A185–200.
- Render, J., Ebert, S., Burkhardt, C., Kleine, T., and Brennecka, G. A. 2019. Titanium Isotopic Evidence for a Shared Genetic Heritage of Refractory Inclusions from Different Carbonaceous Chondrites. *Geochimica et Cosmochimica Acta* 254: 40–53.
- Rubin, A. E., Breen, J. P., Isa, J., and Tutorow, S. 2017. NWA 10214—An LL3 Chondrite Breccia with an Assortment of Metamorphosed, Shocked, and Unique Chondrite Clasts. *Meteoritics & Planetary Science* 52: 372–90.
- Rubin, A. E., Trigo-Rodríguez, J. M., Kunihiro, T., Kallemeyn, G. W., and Wasson, J. T. 2005. Carbon-Rich Chondritic Clast PV1 from the Plainview H-Chondrite Regolith Breccia: Formation from H3 Chondrite Material by Possible Cometary Impact. *Geochimica et Cosmochimica Acta* 69: 3419–30.
- Schrader, D. L., Franchi, I. A., Conolly, H. C., Jr., Greenwood, R. C., Lauretta, D. S., and Gibson, J. M. 2011. The Formation and Alteration of the Renazzo-Like Carbonaceous Chondrites I: Implications of Bulk-Oxygen Isotopic Composition. *Geochimica et Cosmochimica Acta* 75: 308–25.
- Sharp, Z. D., Gibbons, J. A., Atudorei, V., Pack, A., Sengupta, S., Shock, E. L., and Knauth, L. P. 2016. A Calibration of the Triple Oxygen Isotope Fractionation in the SiO₂–H₂O System and Applications to Natural Samples. *Geochimica et Cosmochimica Acta* 186: 105–19.
- Shrbený, L., Borovička, J., Spurný, P., Krzesińska, A. M., Tymiński, Z., and Kmiecik, K. 2022. Analysis of the Daylight Fireball of July 15, 2021, Leading to Meteorite Fall and Find near Antonin, Poland, and Description of the Recovered Meteorite. *Meteoroids 2022 Virtual Conference*, Abstract #6058.
- Slavik, F., and Spencer, L. J. 1928. Place-Names of Mineral-Localities in Central Europe. *Mineralogical Magazine* 21: 441–78.
- Spurný P. 2016. Instrumentally Documented Meteorite Falls: Two Recent Cases and Statistics from all Falls. In *Asteroids: New Observations, New Models*, edited by S. Chesley, A. Morbidelli, R. Jedicke, and D. Farnocchia. Proceedings IAU Symposium 318. Cambridge: Cambridge University Press. pp. 69–79.
- Spurný, P., Borovička, J., Baumgarten, G., Haack, H., Heinlein, D., and Sørensen, A. N. 2017. Atmospheric Trajectory and Heliocentric Orbit of the Ejby Meteorite Fall in Denmark on February 6, 2016. *Planetary and Space Science* 143: 192–8.
- Spurný P., Borovička J., Haloda J., Shrbený L., and Heinlein D. 2016. Two Very Precisely Instrumentally Documented Meteorite Falls: Žďár Nad Sázavou and Stubenberg—Prediction and Reality (Abstract #6221). *Meteoritics & Planetary Science* 51.
- Spurný P., Borovička J., and Shrbený L. 2020. The Zďar nad Sázavou Meteorite Fall: Fireball Trajectory, Photometry, Dynamics, Fragmentation, Orbit, and Meteorite Recovery. *Meteoritics & Planetary Science* 55: 376–401.
- Stelzner, T., Heide, K., Bischoff, A., Weber, D., Scherer, P., Schultz, L., Happel, M., et al. 1999. An Interdisciplinary Study of Weathering Effects in Ordinary Chondrites from the Afer Region, Algeria. *Meteoritics & Planetary Science* 34: 787–94.
- Stepniowski, M., Borucki, J., Durakiewicz, T., Giro, L., and Sharp, Z. D. 2000. Preliminary Study of a New Enstatite Meteorite from Zakłodzie (Southeast Poland). *Meteoritics & Planetary Science* 35: A152–3.
- Stöffler, D., Hamann, C., and Metzler, K. 2018. Shock Metamorphism of Planetary Silicate Rocks and Sediments: Proposal for an Updated Classification System. *Meteoritics & Planetary Science* 53: 5–49.
- Stöffler, D., Keil, D., and Scott, E. R. D. 1991. Shock Metamorphism of Ordinary Chondrites. *Geochimica et Cosmochimica Acta* 55: 3845–67.
- The Meteoritical Bulletin. 2022. Accessed May 15, 2022. <https://www.lpi.usra.edu/meteor/about.php>.
- Trinquier, A., Elliott, T., Ulfbeck, D., Coath, C., Krot, A. N., and Bizzarro, M. 2009. Origin of Nucleosynthetic Isotope Heterogeneity in the Solar Protoplanetary Disk. *Science* 324: 374–6.
- Ward, D., Bischoff, A., Roszjar, J., Berndt, J., and Whitehouse, M. J. 2017. Trace Element Inventory of Meteoritic Ca-Phosphates. *American Mineralogist* 102: 1856–80.
- Wostbrock, J. A., Cano, E. J., and Sharp, Z. D. 2020. An Internally Consistent Triple Oxygen Isotope Calibration of Standards for Silicates, Carbonates and Air Relative to VSMOW2 and SLAP2. *Chemical Geology* 533: 119432.
- Zhang, J., Dauphas, N., Davis, A. M., Leya, I., and Fedkin, A. 2012. The Proto-Earth as a Significant Source of Lunar Material. *Nature Geoscience* 5: 251–5.
- Zhang, J., Dauphas, N., Davis, A. M., and Pourmand, A. 2011. A New Method for MC-ICPMS Measurement of Titanium Isotopic Composition: Identification of Correlated Isotope Anomalies in Meteorites. *Journal of Analytical Atomic Spectrometry* 26: 2197–205.
- Zolensky, M., Herrin, J., Mikouchi, T., Ohsumi, K., Friedrich, J., Steele, A., Rumble, D., et al. 2010. Mineralogy and Petrography of the Almahata Sitta Ureilite. *Meteoritics & Planetary Science* 45: 1618–37.
- Zolensky, M. E., and Ivanov, A. 2003. The Kaidun Microbreccia Meteorite: A Harvest from the Inner and Outer Asteroid Belt. *Chemie der Erde—Geochemistry* 63: 185–246.
- Zolensky, M. E., Ivanov, A. V., Yang, S. V., Mittlefehldt, D. W., and Ohsumi, K. 1996. The Kaidun Meteorite: Mineralogy of an Unusual CM1 Lithology. *Meteoritics & Planetary Science* 31: 484–93.